

# The drag force on spheres in thin jets

By R. S. NEVE, R. NELSON AND P. KOTSIPOULOS

Department of Mechanical Engineering, The City University, London

(Received 20 May 1980 and in revised form 8 August 1980)

The prediction of drag force on spheres whose diameters are comparable to or greater than the dimensions of jets to which they are exposed is found to be much more difficult than in the more usual 'fully immersed' cases. Experimental results show considerable scatter but prediction guidelines are given in the paper. In Reynolds-number terms all results are considered to be supercritical ones because of the typically very high turbulence intensities in the mixing regions of jets.

---

## 1. Introduction

The variation with Reynolds number and Mach number of the drag coefficient for a sphere has been well documented in scientific literature and, provided the sphere concerned is in an infinite fluid, predictions of drag force for a given sphere, fluid and speed can confidently be made. In some industrial sorting operations, however, an unacceptable object is rejected by being hit by an air jet of rectangular or circular cross-section having a depth or diameter less than the principal dimension of the object to be deflected. In this case therefore a prediction of deflecting force based on the usual drag coefficient and frontal area is likely to be seriously in error. The problem is only slightly less intractable if the object approximates in shape to a sphere and if its centre coincides with the jet axis. These idealizations have had to be made in this paper.

When jet and sphere have comparable cross-sectional dimensions, the problem resembles that encountered by aeronautical engineers evaluating drag coefficients of models in wind tunnels. A blockage correction must be applied because in a closed wind tunnel the streamline separation is artificially lowered because of the solid walls whereas in an open section tunnel the streamline separation is too great because of the constant pressure boundary. The correction to be applied in these two cases are consequently of opposite sign. A previous paper by Achenbach (1974) has dealt with spheres in circular-section closed wind tunnels but the work reported in the present paper deals with spheres in finite circular and rectangular jets and is believed to be unique.

## 2. Theoretical considerations

### 2.1. *Spheres in circular jets*

The most important parameters affecting the drag force  $F$  on a sphere of diameter  $d$  on the centre-line of a jet issuing from a circular nozzle of diameter  $D$  are the jet speed at the nozzle  $u_0$ , the downstream distance  $x$  of the sphere nose from the nozzle and the jet properties of density  $\rho$ , kinematic viscosity  $\nu$  and local speed of sound  $a$ . Three other very important variables are the surface roughness of the sphere, its sphericity and the

relative intensity of turbulence in the flow  $I$ , defined as the r.m.s. value of the fluctuating velocity component divided by the time mean value of fluid velocity at that point.

A straightforward dimensional analysis of the problem using Buckingham's method would require the selection of three variables with which to render the others dimensionless. If  $\rho$ ,  $u_0$  and  $D$  are chosen then the dimensionless drag force  $F/\rho u_0^2 D^2$  can easily be shown to be a function of the geometrical ratios  $x/D$  and  $d/D$ , the Reynolds number, Mach number, relative intensity of turbulence, surface-roughness parameter and sphericity.

The number of these functions needing to be considered can be minimized by making the spheroids as near spherical as possible and by surface polishing to the extent that hydraulic smoothness might reasonably be assumed. The well-known drop in drag force which suddenly occurs when the surface boundary layers change from laminar to turbulent form is then likely to appear at a Reynolds number of about  $3.7 \times 10^5$ , as given by Achenbach (1974). Unfortunately, the value of  $Re$  at which this drop occurs is also a function of turbulence intensity, the former decreasing as the latter increases.

In their investigations of heat transfer from spheres in moving fluids, Lavender & Pei (1967) found it useful to define a 'turbulent Reynolds number'  $Re_T$  as the product of  $Re$  and  $I$ . Their results show that, at a value of  $Re_T$  of about 1000, drag coefficient decreases suddenly and heat transfer begins to increase with  $Re$  and they attribute this to passing through the usual critical-Reynolds-number condition. Their method of measuring drag is unspecified and experimental scatter is considerable so the value of 1000 should perhaps be treated with care. Results from other sources suggest the critical value of  $Re_T$  should be higher. If the critical Reynolds numbers quoted by Achenbach (1972, 1974) are multiplied by his given turbulence intensities, a value of around 1600 is obtained. If results given by Pope & Harper (1966) are treated in the same way, it is seen that the critical value of  $Re_T$  increases with  $I$ , tending towards a limiting value of about 3850.

The point of this argument is that in a jet, where the turbulence intensity is characteristically very high, the product of Reynolds number (based on jet speed in the nozzle) and  $I$  is likely always to be well above 3850, indicating the likelihood of a turbulent boundary layer on an immersed sphere, even if the Reynolds number itself is at a subcritical value in the Achenbach sense. Detailed investigations of jet turbulence have been made by Davies, Fisher & Barratt (1963), Goldschmidt & Eskinasi (1966), Heskestad (1965) and Miller & Comings (1957). All seem to agree that in the regions of considerable shearing action just outside the inviscid core of a jet and downstream, values of  $I$  as high as 0.25 can be encountered. This means that a sphere having a subcritical value of  $Re$  of  $10^5$  would experience a supercritical value of  $Re_T$  of  $2.5 \times 10^4$  if placed in the appropriate regions of a jet. It seems fair to assume therefore that, provided a sphere is not tested in a situation where  $Re_T$  is less than about 5000, the boundary layers may be taken to be turbulent and Reynolds number need not thereafter be considered as a variable since the results of Achenbach (1972) show that under these conditions  $C_D$  approaches a constant value of 0.2.

Spheres were tested at various Mach numbers by Naumann (1953) who showed that drag coefficient  $C_D$  and critical Reynolds number were unaffected by Mach number up to about  $M = 0.3$  and that thereafter both increased slightly up to  $M = 0.5$ . In the tests reported here, Mach number never exceeded 0.53 at the nozzle and was generally

between 0.1 and 0.3 so that this parameter will not hereafter be considered an important variable. The changes involved would have been within experimental error in any case.

With the above simplifications therefore we are left with

$$F/\rho u_0^2 D^2 = \phi[(x/D), (d/D)]. \quad (1)$$

If the denominator of the left-hand side is multiplied by  $\frac{1}{4}\pi$ , it becomes the jet momentum flux  $J$ , assuming very thin boundary layers in the nozzle. This is an attractive normalizing quantity because it should remain constant with downstream travel, provided the jet is not subject to an ambient pressure gradient.

The task of analysing experimental results would be made easier if the general statement represented by the right-hand side of (1) could be represented by two functions, one being a function of  $x/D$  only, the other of  $d/D$  only. This simplification could only be justified afterwards by results. We have now therefore

$$F/J = \phi_1(x/D) \phi_2(d/D), \quad (2)$$

where any pure number constants have been absorbed into one of the  $\phi$  functions. For convenience,  $\phi_2$  is chosen for this. The form of these functions can be found only by experiment, however.

## 2.2. Spheres in rectangular jets

All the foregoing comments apply equally well to spheres in thin rectangular jets except that  $D$  is replaced by a nozzle height  $h$  and width  $w$ . The downstream position of the sphere can now be related to either  $h$  or  $w$ , as can the sphere diameter. If  $h$  is taken to be smaller than  $w$ , then experience would suggest selecting  $h$  since the extent of the jet's inviscid core will depend more closely on this quantity. Equation (1) might therefore be rewritten as

$$F/J = \psi_1(x/h) \psi_2(h/d) \psi_3(w/d) \quad (3)$$

with the same provisos as apply to (2).

The functions  $\psi_2$  and  $\psi_3$  are in reality the same, if gravity is ignored, since Nature will not prefer one direction to an orthogonal one, so that even if  $h$  and  $w$  are widely different they are nevertheless at two extremes of the same functional relationship. Equation (3) therefore reduces to

$$F/J = \psi_1(x/h) \psi_2(h/d) \psi_2(w/d), \quad (4)$$

where once again any pure number constants have been absorbed into  $\psi_2$ .

This project was therefore concerned with investigating the drag on spheres in thin jets in terms of (2) and (4), ensuring that the product of local Reynolds number and relative turbulence intensity was always in the supercritical region. However, there was one case, mentioned below, where doubt must be raised about satisfying this criterion.

## 3. Experimental arrangement

Five wooden spheres were used in this project: their diameters were 31, 63, 73, 97 and 115 mm. All were finished to a high standard, varnished and polished so that an assumption of hydraulic smoothness would be justified. Each had a threaded hole to

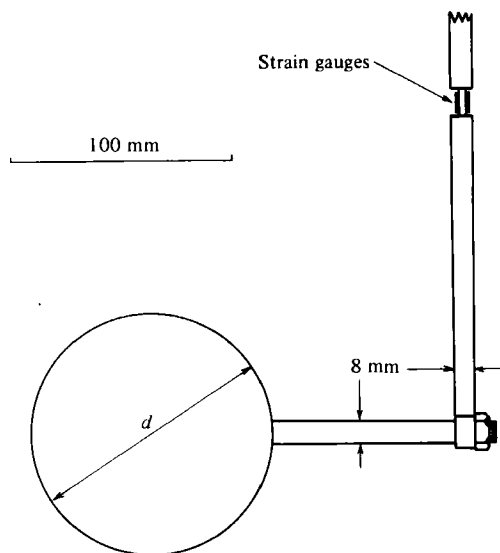


FIGURE 1. Strain-gauge cantilever force transducer.

fit the sting of a strain-gauged cantilever force transducer (figure 1). The strain gauges were connected to a Wheatstone half-bridge, the unbalanced voltage from which was fed to a time-averaging digital voltmeter. Calibration was against known static forces.

The sting was of 8 mm diameter and in the case of the smallest sphere this gives a diameter ratio of 0.26. This is unlikely to have caused a substantial  $C_D$  change since the sting diameter is probably much less than that of the wake. In cases where sting-mounted bodies are being tested in wind tunnels, the ratio of sting-to-body diameters is usually not less than about 0.6 and Pope & Harper (1966) state that there is then a slight reduction in measured  $C_D$  because the flow just outside the wake has a body to which to attach.

As stated later, the smallest sphere was used only in the case of circular jets and in the case where the jet diameter was larger than the sphere's, the  $C_D$  values will be seen to be tending towards those of Achenbach.

The force transducer was attached to an  $x$ - $y$ - $z$  traversing gear bolted to the floor. The spheres could thus be manoeuvred on to the jet centre-line at any downstream station, the centre-line being located by Pitot tube. It was found that central positioning needed to be accurate to better than 1 mm of radius error.

Circular jets were produced from four nozzles, each being fitted in turn into the side of a large air tank. The three smaller ones were properly contoured convergent circular nozzles having exit diameters of 3.17, 12.5 and 19.1 mm. The largest of the four was a sharp-edged orifice so a vena contracta area correction of 0.62 has been used in specifying its jet diameter as 45.7 mm. The air tank was supplied via a filter and pressure regulator from a large compressor. No supply pressure variations were encountered during testing.

For rectangular jets, two arrangements were available. For producing jets initially 100 mm wide and 8 mm deep, the tank described above was modified to allow the fitting of a rectangular nozzle having contoured converging upper and lower lips and parallel side plates. For producing jets initially 760 mm wide, a completely

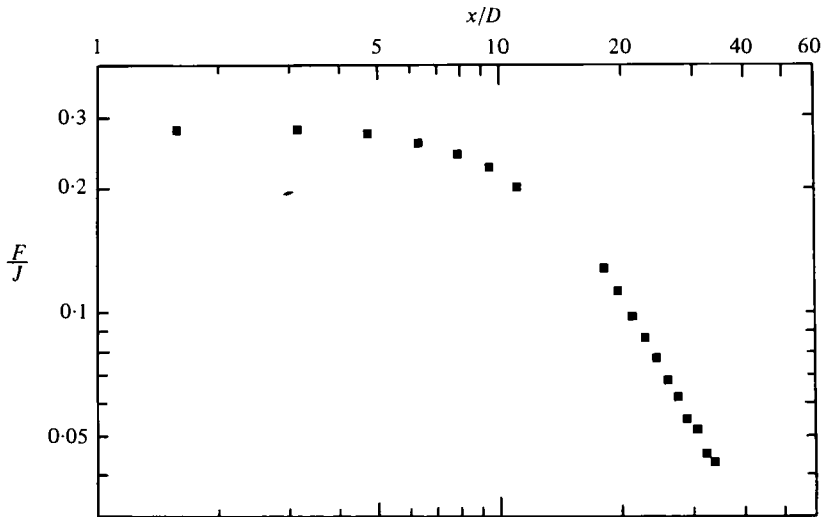


FIGURE 2. Variation of  $F/J$  with downstream distance,  $d = 31$  mm,  $D = 12.7$  mm.

different rig was employed consisting of a large wooden plenum chamber measuring approximately one metre square in plan view and 2 m high, fed from its own blower. In one of the vertical walls of this chamber were two horizontal converging-nozzle contours, the upper one being moveable vertically to give  $h$  values up to 30 mm.

The flow involved in these tests was inherently an unsteady one because of vortex shedding, especially so in the case of rectangular jets because axisymmetry was lost. The worst excesses of this unsteadiness were, however, minimized using an averaging digital voltmeter, as mentioned above. Even then, an averaging period of 10 s was generally required and in the more favourable case of circular jets the average values obtained over many spells of 10 s were within 6% of their arithmetic mean. The scatter with rectangular jets was generally worse, as will be seen in the next section, but, in assessing the results, the flow unsteadiness should be constantly borne in mind.

## 4. Discussion of results

### 4.1. Spheres in circular jets

Results were obtained by testing a particular sphere and nozzle at various axial locations of the former. This process was then repeated for all spheres and nozzles.

By way of illustration, the  $F/J$  values obtained with the 31 mm sphere and 12.7 mm nozzle are shown in figure 2. At larger downstream distances, the values of  $F/J$  fall off with distance approximately as  $(x/D)^{-1.8}$ , whereas close to the nozzle they become constant, clearly showing the influence of the jet's inviscid core, where velocity is constant. Tests were not attempted too close to the nozzle because blockage by the sphere became apparent. Also, tests could not be conducted at very large distances, where the power of  $x/D$  might be expected to approach  $-2$ , because the experimental inaccuracy became a significant proportion of the measurable drag force.

It is instructive to consider at this point the variation with downstream distance of  $C_D$  based on the frontal area of the spheres and the jet velocity  $u$  that would have

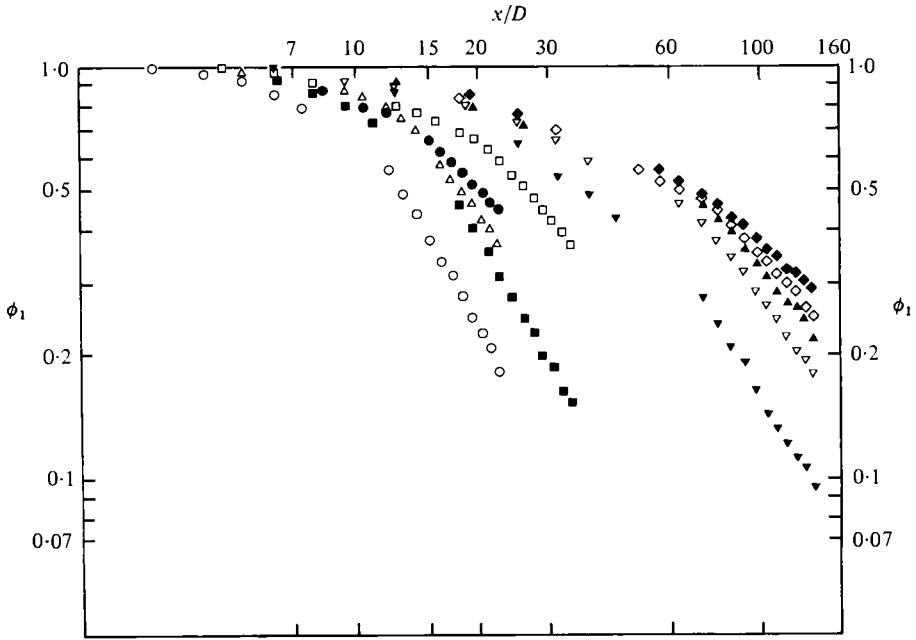


FIGURE 3. Variation of function  $\phi_1$  with downstream distance for the following ratios of  $d/D$ :  $\circ$ , 1.62;  $\blacksquare$ , 2.44;  $\triangle$ , 3.80;  $\bullet$ , 5.10;  $\square$ , 7.64;  $\blacktriangledown$ , 9.78;  $\triangledown$ , 19.7;  $\blacktriangle$ , 23.0;  $\diamond$ , 30.6;  $\blacklozenge$ , 36.3.

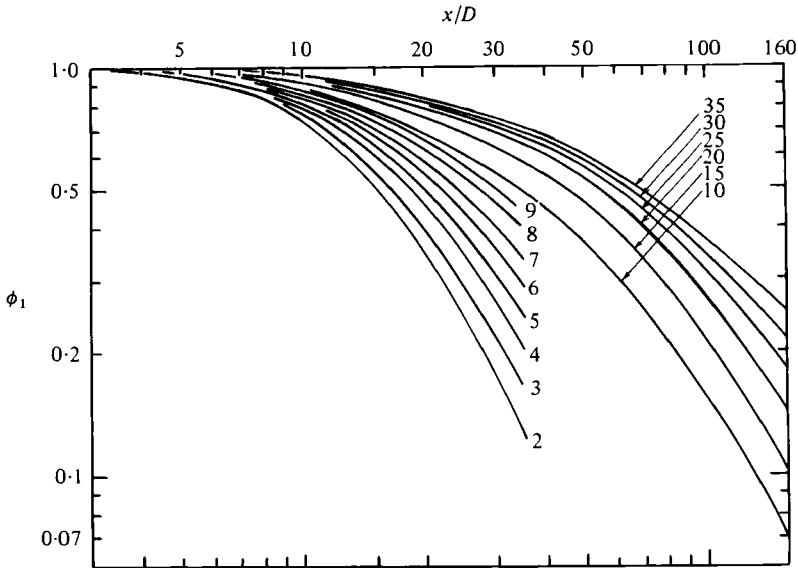


FIGURE 4. Interpolated and smoothed version of figure 3. (The numbers indicate the  $d/D$  ratios.)

obtained at the nose of the sphere had the latter not been present to modify the flow.  $C_D$  is easily shown to be  $2(F/J)(u_0/u)^2(D/d)^2$  for a circular jet case so that, with  $(F/J)$  varying as  $x^{-1.8}$  outside the core region and  $(u_0/u)^2$  varying as  $x^2$ , their product is a weak function of  $x$ , increasing as  $x^{0.2}$ . This would mean that, with downstream travel,

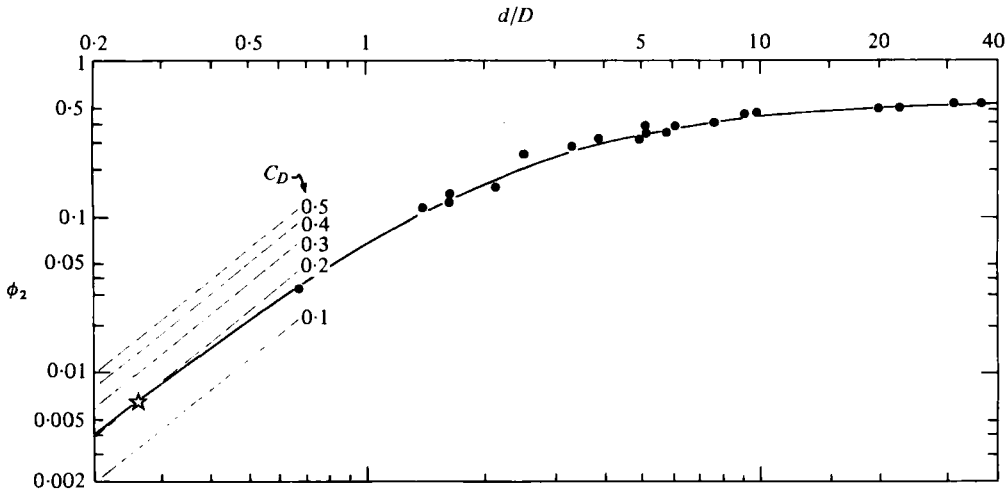


FIGURE 5. Variation of function  $\phi_2$  with diameter ratio.  
 —, equation (5); ☆, Achenbach (1972).

$C_D$  would increase slightly, probably because the jet is becoming wider and the distribution of turbulence intensity across the face of the sphere is therefore changing.

When using the largest jet (45.7 mm) and smallest sphere (31 mm) close to the nozzle, an axial traverse point could be found where the drag force suddenly jumped to at least double its previous value. This was almost certainly because the sphere had completely entered the inviscid core and was subject to much lower turbulence intensities than outside. The Reynolds number for this condition was  $2.15 \times 10^5$ , well below the critical value commonly accepted. A laminar boundary layer therefore probably existed on the sphere under these conditions and this justifies the assumption made earlier that all results except this one are in the supercritical region since no other sphere exhibited this phenomenon. There is obviously, however, scope for further work here.

For the purposes of finding  $\phi_1(x/D)$  in equation (2), the value of the left-hand end of figure 2 can be set at unity and the plot then becomes  $\phi_1$  versus  $x/D$ . This can be repeated for all spheres and nozzles and the result is shown in figure 3. Not all points are included for reasons of clarity. The function clearly depends on  $d/D$  and a smoothed, interpolated version is shown in figure 4. Extrapolation beyond justifiable limits has not, however, been attempted.

The inability of equation (2) to replace (1) is clear from figure 3, since the values of  $\phi_1$  depend on  $d/D$  as well as on  $x/D$ . It would be more realistic therefore to modify the equation to

$$F/J = \phi_1(x/D, d/D) \phi_2(d/D). \tag{2a}$$

It can be seen from (2a) that a consequence of setting  $\phi_1$  at unity for small  $x/D$  values is that  $F/J$  then represents the value of  $\phi_2(d/D)$  for that ratio of  $d/D$ . This can be repeated for all spheres and all nozzles to give a plot of  $\phi_2$  versus  $d/D$ ; this is shown in figure 5. The function  $\phi_2$  is analogous to the blockage correction that would need to be applied to the drag of an object tested in a finite open-section wind tunnel. At one extreme, where the sphere diameter is more than 36 times that of the jet, the

drag force tends to slightly more than one half the jet momentum flux; at the other extreme, the experimental values seem to point towards Achenbach's value, obtained with a jet: sphere diameter ratio of about 3.85 and corresponding to a drag coefficient at high supercritical Reynolds numbers of 0.20. The line

$$\phi_2(d/D) = 0.563/\{1 + 2.25(D/d) + 5.075(D/d)^2\} \quad (5)$$

is seen to be a satisfactory fit to the experimental points and suggests that for very thin jets and large spheres the drag force tends to 56.3% of the jet momentum flux whereas for large jets and small spheres the value of  $C_D$  tends to 0.222.

In this latter case, it should be emphasized again that only clearly supercritical values have been used to plot figure 5; the subcritical results obtained with the 31 mm sphere in an inviscid core would have caused the left-hand side of the curve to tend towards a  $C_D$  value of about 0.5.

#### 4.2. Spheres in rectangular jets

Although the 760 × 30 mm nozzle produced jets which might be considered infinite in lateral extent (especially as the spheres were never placed further away than about 500 mm), the 100 × 8 mm nozzle produced jets which could certainly not be considered infinite plane ones. Traverses were therefore undertaken to establish velocity profiles in the latter case, using a Pitot tube.

From traverses in the direction parallel to the  $h$  dimension, the velocity profiles downstream of about  $x = 8h$  were found to be broadly similar and of the usual Gaussian form whereas from traverses parallel to the  $w$  dimension the profiles were found to be flat-topped at all stations tested (up to about  $30h$ ). This latter point is not surprising since these traverses were all at distances less than about  $6w$ . The lateral extent of the flat tops was, however, decreasing with downstream travel, in accordance with the concept of a diminishing inviscid core.

In both traverse directions, the centre-line velocity  $U_c$  was of course common and was found to conform closely to the equation

$$U_c/U_0 = 2.4(x/h)^{-0.47},$$

which is typical of those quoted in the many references on plane jets. Details are given in Grantham (1977).

In testing the spheres in rectangular jets, results for the 31 mm sphere were discarded altogether as being thoroughly unreliable. It proved impossible to obtain repeatable force values, almost certainly because the sphere was sometimes in a supercritical flow regime and sometimes in a subcritical one. The combinations of nozzle height, sphere diameter and jet speed made it difficult to overcome this problem. Figure 6 therefore contains force results only for the four larger spheres, normalized in the same way as for figure 3, to give  $\psi_1(x/h)$  versus  $x/h$ . The function now appears to be a unique one, the points once again showing a plateau at the left-hand end corresponding to positions in the inviscid core and passing to a line of gradient  $-0.74$  through a short transition region. The break point appears to be at about  $x = 8h$  for all spheres.  $\psi_1$  can be approximated by the equation

$$\psi_1(x/h) = 4.67(x/h)^{-0.74} \quad (6)$$

if  $x/h$  is greater than about 10 and equals unity if  $x/h$  is less than about 6.

As in the case of circular jets, it is worth while noting how  $C_D$  varies with  $x$ . For a



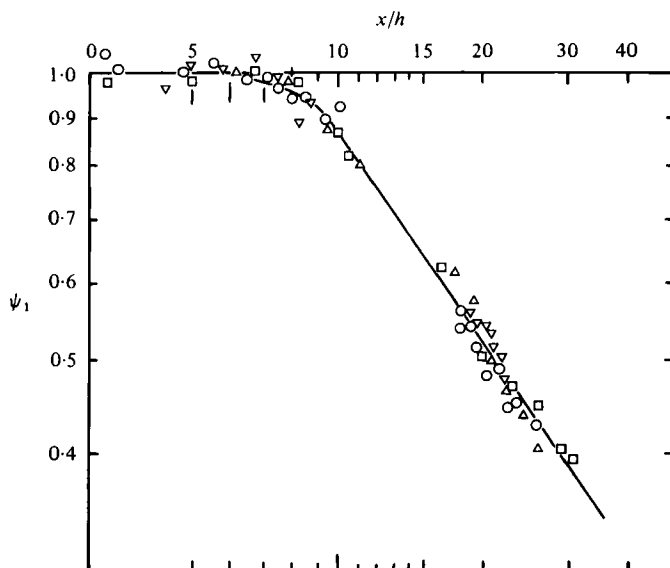


FIGURE 6. Variation of function  $\psi_1$  with downstream distance for the following values of  $d$  (mm):  $\circ$ , 63;  $\square$ , 73;  $\triangle$ , 97;  $\nabla$ , 115. —, equation (6).

rectangular jet,  $C_D$  is given by  $(8/\pi)(F/J)(u_0/u)^2(h/d)(w/d)$  so that for a given jet and sphere  $C_D$  is proportional to  $(F/J)(u_0/u)^2$ . The results just given indicate that, downstream of the core,  $(F/J)$  varies as  $x^{-0.74}$  whereas  $(U_0/U)^2$  varies as  $x^{0.94}$  so their product varies as  $x^{0.2}$ . This is the same as for the circular jets case and almost certainly for the same reason.

In finding the form of the function  $\psi_2$  an assumption is needed. To isolate its value for very small  $h/d$ , testing must take place with a jet of high  $w/h$  ratio (aspect ratio); it may then be reasonably assumed that  $F/J$  is proportional to the ratio of sphere diameter to jet width. That is,

$$F/J = \psi_1(x/h) \psi_2(h/d) K(w/d)^{-1}. \tag{7}$$

If spheres are tested in the region  $x/h < 6$ , then  $\psi_1$  may be assumed equal to unity (figure 6) so that only the last two terms in (7) need be considered. The value of the proportionality constant  $K$  can now be found by assuming that, if  $w$  and  $h$  are very small compared with the sphere diameter, the value of  $F/J$  will be the same as for a circular jet of diameter equal to  $w$  or  $h$ . Equation (5) suggests that under these extreme conditions

$$\psi_2(h/d) \psi_2(w/d) = 0.563$$

so that  $\psi_2$  at very low  $h/d$  values is the square root of 0.563, which is 0.7503. The value of  $K$  is then found by requiring the experimental values of  $\psi_2$  to tend to 0.75 at low  $h/d$  values (figure 7). This method is clearly approximate but the results scatter does not warrant a more rigorous approach. The mean value of  $K$  for the four spheres was found to be 0.484 and the asymptote  $0.484(w/d)^{-1}$  has been superimposed on figure 7 for higher  $w/d$  or  $h/d$  values. The experimental points (closed symbols) show a clear trend towards this asymptote.

Since the line has a slope of minus one, a first-order equation could be employed to

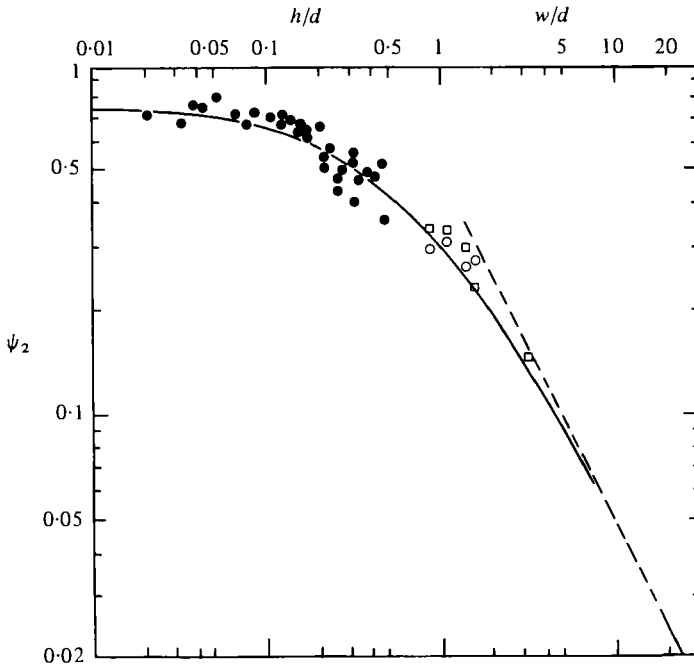


FIGURE 7. Variation of function  $\psi_2$  with  $h/d$  and  $w/d$ . —, equation (8); - - -, asymptote. Closed symbols,  $w = 760$  mm; open symbols,  $w = 100$  mm;  $\square$ , Grantham (1977),  $w = 100$  mm.

obtain a 'fairing in' curve between the two extremes of the function and that equation is

$$\psi_2 = 0.7503 / \{1 + 1.55(h/d)\}. \quad (8)$$

All the above results were obtained with the 760 mm wide jet but four further points can be obtained on figure 7 using results from the 100 mm wide nozzle and the four larger spheres, equation (8) being used to correct for  $\psi_2(h/d)$ . The  $w/d$  values range from 0.869 for the 115 mm sphere to 1.587 for the 63 mm one and these results clearly follow the line represented by (8). Their scatter is almost as poor as for the other points on figure 7 but, bearing in mind the unsteady nature of the flow and the concomitant difficulties in measuring the drag forces, this is not surprising. Also superimposed on figure 7 are results obtained by Grantham (1977) using all five spheres and a mechanical balance for drag measurement. Allowing once again for experimental scatter, they agree well with the results obtained with the strain-gauged force transducer and the number of results going to make up figure 7 suggests that this figure can be treated with some confidence.

#### 4.3. Accuracy

Experimental accuracy in these tests was not high. Positioning of the sphere exactly on the jet centre-line and measurement of a time-averaged drag force were the points of major concern and these have been commented upon already. The measurement of  $x$  and  $J$  were relatively much more accurate. Although scatter is high, especially in the case of rectangular jets, it is suggested that, in view of the number of results obtained, it would be justifiable to quote a probable error of  $\pm 10\%$  for predicted drag forces obtained from these figures.

## 5. Conclusions

The prediction of drag force on a sphere exposed to a thin jet has been found to be more difficult and less trustworthy than in 'fully immersed' cases. For circular jets, equation (2a) can be used with  $\phi_1$  obtained from figure 4 and  $\phi_2$  from figure 5. For rectangular jets, equation (4) can be used, with figure 6 providing the values of  $\psi_1$  and figure 7 giving both required values of  $\psi_2$ .

In all cases experimental points scatter has been found to be considerable and it is unlikely that an accuracy of better than about  $\pm 10\%$  is justifiable for any drag predictions.

All results quoted are considered to be supercritical ones in the Reynolds-number sense because of the very high turbulence intensities encountered in jets. In cases where the sphere is totally engulfed by the jet's inviscid core, a higher drag is encountered and further work is needed in predicting the drag under these subcritical conditions.

The authors wish to express their gratitude to the Science Research Council for financial support for this project in the form of a Research Grant.

## REFERENCES

- ACHENBACH, E. 1972 Experiments on flow past spheres at very high Reynolds numbers. *J. Fluid Mech.* **54**, 565-575.
- ACHENBACH, E. 1974 The effects of surface roughness and tunnel blockage on the flow past spheres. *J. Fluid Mech.* **65**, 113-125.
- DAVIES, P. O. A. L., FISHER, M. J. & BARRATT, M. J. 1963 The characteristics of the turbulence in the mixing region of a round jet. *J. Fluid Mech.* **15**, 337-367.
- GOLDSCHMIDT, V. & ESKINAZI, S. 1966 Two phase turbulent flow in a plane jet. *Trans. A.S.M.E. E, J. Appl. Mech.* **33**, 735-747.
- GRANTHAM, P. J. 1977 The drag force on partially immersed spheres. M.Sc. thesis, The City University, London (Dept. of Mech. Engineering).
- HESKESTAD, G. 1965 Hot wire measurements in a plane turbulent jet. *Trans. A.S.M.E. E, J. Appl. Mech.* **32**, 721-734 (erratum: **33**, 710).
- LAVENDER, W. J. & PEI, C. P. 1967 The effect of fluid turbulence on the rate of heat transfer from spheres. *Int. J. Heat Mass Transfer* **10**, 529-539.
- MILLER, D. & COMINGS, E. 1957 Static pressure distribution in the free turbulent jet. *J. Fluid Mech.* **3**, 1-16.
- NAUMANN, A. 1953 Luftwiderstand von Kugeln bei hohen Unterschallgeschwindigkeiten. *Allgem. Wärmetechnik* **4**, 217-221.
- POPE, A. & HARPER, J. J. 1966 *Low Speed Wind Tunnel Testing*. Wiley.